Int. J. Electrochem. Sci., 6 **(2011)** 2131 - 2148

International Journal of
ELECTROCHEMICAL
SCIENCE
www.electrochemsci.org

Corrosion of Magnesium/Manganese Alloy in Chloride Solutions and its Inhibition by 5-(3-Aminophenyl)-tetrazole

El-Sayed M. Sherif [1,2,*], *Abdulhakim A. Almajid* [1,3]

[1] Center of Excellence for Research in Engineering Materials (CEREM), College of Engineering, King Saud University, P. O. Box 800, Al-Riyadh 11421, Saudi Arabia
[2] Electrochemistry and Corrosion Laboratory, Department of Physical Chemistry, National Research Centre (NRC), Dokki, 12622 Cairo, Egypt
[3] Department of Mechanical Engineering, College of Engineering, King Saud University, P.O. Box 800, Al-Riyadh 11421, Saudi Arabia
[*]E-mail: esherif@ksu.edu.sa

Received: 20 April 2011 / *Accepted:* 12 May 2011 / *Published:* 1 June 2011

The corrosion and corrosion inhibition of Mg/Mn alloy in 3.5% NaCl solutions by 5-(3-aminophenyl)-tetrazole (APT) after different exposure intervals have been studied. The work was carried out using conventional electrochemical, impedance, and gravimetric measurements and complemented by scanning electron microscopy (SEM) and X-ray analyzer (EDX) investigations. Cyclic polarization, chronoamperometry and electrochemical impedance spectroscopy measurements after 60 min and 6 days indicated that the corrosion of Mg/Mn alloy decreases with increasing exposure time. This effect was significantly enhanced with the presence and upon the increase of APT molecules in the chloride solution. Weight loss tests after varied exposure periods (5–25 days) showed that the weight loss of the alloy increases and the corrosion rate decreases with time. APT provided an inhibition efficiency of circa 55% at 10^{-3}M increased to about 91% with $5x10^{-3}$ M in 25 days.

Keywords: Chloride solutions, conventional electrochemical techniques, corrosion, gravimetric tests, impedance, magnesium alloys, SEM/EDX investigations

1. INTRODUCTION

Due to the low density, good heat dissipation, good damping, and good electro-magnetic shield, magnesium alloys have the extensive and increasing applications because of their lightest of all structural metallic materials [1-4]. Although, magnesium alloys form oxide layer on their surfaces, this layer non compact and leads to a poor corrosion resistance especially in chloride containing environments. When a magnesium alloy contacts aggressive medium contains Cl^- ions, Cl^- ions will

penetrate the oxide layer reaching the surface of the alloy then reacting with the metal substrate, which leads to the occurrence of corrosion. The high corrosion trend is also predicted due to the high electron negative potential of Mg. Moreover, impurities and second phases act as active cathodic sites causing local galvanic acceleration of corrosion of the matrix [5]. The corrosion performance of magnesium alloys in sodium chloride solutions is affected among other things by alloying elements, precipitations, microstructure, and grain size [6–8]. The alloys containing low amounts of iron, copper and nickel are more corrosion resistant. These elements act as active cathodes with small hydrogen overvoltage and result in dissolution of the magnesium matrix. Therefore, a surface treatment for protection against corrosion is usually required for aggressive electrolytes exposure [9-13].

The coatings and surface treatments used in industry to protect magnesium alloys are, oils and waxes for temporary protection; chemical-conversion coatings for temporary protection or paint base; anodized coatings for wear resistance as well as a superior paint base; paints and powder coatings used for corrosion protection and appearance; metallic plating is good for appearance, surface conductivity, solderability and limited corrosion protection; and adding corrosion inhibitors for increasing the surface resistance by isolating from being in contact with the corrosive environment [8, 9–13]. Chemical conversion coatings, for instance, can provide limited stand-alone protection for interior environment applications [8, 9–13]. Anodised coatings are inherently porous, and unless they are properly sealed with paint or resin, are not suitable for exposure to corrosive environments. Metallic coatings are restricted to special applications, because of the high processing costs involved in deposition [10].

A great number of investigations have been devoted to the protection of magnesium [8] but very little work has been seldom involved on the adding corrosion inhibitors. The use of corrosion inhibitors is one of the most important methods for the protection of metals and alloys against corrosion in harsh environments [14–22]. Among those, organic compounds containing polar groups including nitrogen, sulfur, and oxygen and heterocyclic compounds with polar functional groups and/or conjugated double bonds have been reported to be good corrosion inhibitors [14-23]. The inhibition of these compounds is usually attributed to their interaction with the metal surface via their adsorption. The adsorption of an inhibitor onto a metal surface depends on the nature as well as the surface charge of the metal, the adsorption mode, its chemical structure, and the type of the electrolyte solution [24].

For the metals widely employed in the industry such as iron, copper and aluminum, adding corrosion inhibitors is an effective and convenient method to decrease the corrosion rate [14–25]. For magnesium and its alloys, there are very few publications on their corrosion inhibitors and only few inhibitors such as the salts of F^- [14, 26], $Cr_2O_7^{2-}$ [26], 8-hydroxyquinoline [27], alkyl carboxylate [28] and so on, are involved. The inhibition of magnesium engine block in commercial coolants by KF as an inhibitor to reduce the corrosivity of these coolants to magnesium alloys have been reported by Song and StJohn [25]. Mesbah et al. [28] have studied the inhibition of magnesium corrosion in sodium decanoate solutions by alkyl carboxylate and found that the surface can be protected due to the hydrophobic features of the aliphatic chains of the organic inhibitor. Yang et al. [29] studied the change of polarization current density of AZ61 magnesium alloy in alkali aqueous solution with 5mmol/L sodium dodecylsulphate, phytic acid, ethylenediamine tetraacetic acid, p-nitro-benzene-azo-

resorcinol, acidum tannicum or stearic acid. They found that those organic compounds which could form the inhibitor-magnesium precipitation in aqueous solution could be used as corrosion inhibitors for magnesium alloys to inhibit the increase of polarization current density as well as the dissolution and oxidation of magnesium alloys effectively.

The aim of this paper is to study the corrosion of magnesium in stagnant 3.5% sodium chloride solutions after 60 min and 6 days exposure periods using electrochemical measurements and within 5–25days immersion in the solution using weight-loss data and SEM/EDX investigations. The aim is also extended to study the effect of 5-(3-aminophenyl)-tetrazole (APT) on the inhibition of Mg corrosion at the same conditions. It is worth to mention that APT has shown excellent performance as a corrosion inhibitor for copper [24, 30] and iron [31] in chloride media.

2. EXPERIMENTAL PROCEDURE

2.1. Chemicals and electrochemical cell

5-(3-Aminophenyl)-tetrazole (APT, Alfa-Aesar, 96%), sodium chloride (NaCl, Merck, 99%), and absolute ethanol (C_2H_5OH, Merck, 99.9%) were used as received. A solution of 7.0% sodium chloride (NaCl, Merck, 99%), was prepared by dissolving 140 g of NaCl in 2 L glass flask. The test solution (3.5% NaCl) was prepared from the stock by dilution. An electrochemical cell with a three-electrode configuration was used; a square magnesium electrode (with the chemical composition shown in Table 1 and having 1.2 cm side length and total surface of 1.44 cm^2), a platinum foil, and an Ag/AgCl electrode (in the saturated KCl) were used as the working, counter, and reference electrodes, respectively.

Table 1. Chemical compositions of the magnesium/manganese alloy.

Element	Mn	Al	Si	Cu	Ni	Fe	Others each	Other total	Mg
M1C	0.50-1.3	0.01	0.05	0.02	0.001	0.03	0.05 Max	0.30 Max	Remainder

The Mg rod for electrochemical measurements was prepared by welding a copper wire to a drilled hole was made on one face of the rod; the rod with the attached wire were then cold mounted in resin and left to dry in air for 24 h at room temperature. Before measurements, the other face of the Mg electrode, which was not drilled, was polished successively with metallographic emery paper of increasing fineness up to 1200 grit. The electrode was then cleaned using doubly-distilled water, degreased with acetone, washed using doubly-distilled water again and finally dried with a stream of dry air. In order to prevent the possibility of crevice corrosion during measurement, the interface between sample and resin was coated with Bostik Quickset, a polyacrelate resin.

2.2. Electrochemical methods

Electrochemical experiments were performed by using an Autolab Potentiostat (PGSTAT20 computer controlled) operated by the general purpose electrochemical software (GPES) version 4.9. The cyclic potentiodynamic polarization (CPP) curves were obtained by scanning the potential in the forward direction from -2000 to -800 mV against Ag/AgCl at a scan rate of 3.0mV/s; the potential was then reversed in the backward direction at the same scan rate. Chronoamperometric current-time (CA) experiments were carried out by stepping the potential of the magnesium electrodes at – 1200 mV versus Ag/AgCl. Electrochemical impedance spectroscopy (EIS) data were performed at corrosion potentials (E_{Corr}) over a frequency range of 100 kHz – 100 mHz, with an ac wave of ± 5 mV peak-to-peak overlaid on a dc bias potential, and the impedance data were collected using Powersine software at a rate of 10 points per decade change in frequency. All the electrochemical experiments were recorded for the Mg electrodes after 60 minutes and 6 days immersions in the test electrolytes before measurements. All measurements were also carried out at room temperature in freely aerated solutions.

2.3. Weight-loss measurements

The weight loss experiments were carried out using rectangular magnesium coupons (with the same chemical composition of magnesium rods) having a dimension of 4.0 cm length, 2.0 cm width, and 0.4 cm thickness and the exposed total area of 54.0 cm^2. The coupons were polished and dried as for the case of Mg rods, weighed, and then suspended in 300 cm^3 solutions of 3.5% NaCl in absence and presence of $1x10^{-3}$ and $5x10^{-3}$ M APT for different exposure periods (5–25 days).

2.4. SEM investigation and EDX analysis

The SEM investigation and EDX analysis were obtained for the surface of magnesium specimens after their immersions in 3.5% NaCl solution in absence and presence of 10^{-3} APT for 25 days. The investigations included also the alloy surface after 6 days immersion in sodium chloride solution followed by running the CPP test. The SEM images were carried out by using a JEOL model JSM-6610LV (Japanese made) scanning electron microscope with an energy dispersive X-ray analyzer attached.

3. RESULTS AND DISCUSSION

3.1. Cyclic potentiodynamic polarization (CPP) measurements

The CPP curves for Mg electrode after its immersion for 60 min (1) and 6 days (2), respectively in 3.5% NaCl solutions are shown in Fig. 1. The polarization experiments were carried out in order to obtain the corrosion parameters like corrosion potential (E_{Corr}), corrosion current (j_{Corr}), protection potential (E_{Prot}), polarization resistance (R_P), and corrosion rate (K_{Corr}) of Mg in the test

solution after the different exposure intervals. Although, the cathodic reaction for metals and alloys in aerated near neutral solutions is well known to be the oxygen reduction [15–18], it is the hydrogen evolution for Mg as the electron consumption on magnesium happens by the unloading of hydrogen ions (acidic corrosion),as follows [32],

$$2H^+ + 2e^- = H_2 \quad (1)$$

The source of the hydrogen ions (more exactly the hydronium ion H_3O) is the dissociated water, as shown below;

$$H_2O = H^+ + OH^- \quad (2)$$

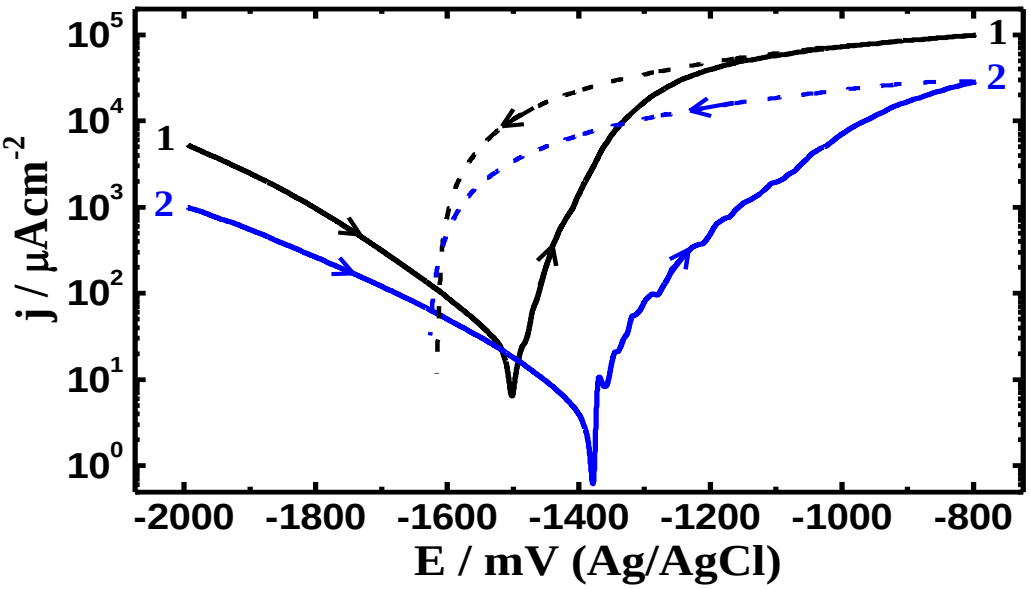

Figure 1. CPP curves obtained for Mg electrode after its immersion in freely aerated stagnant solutions of 3.5% NaCl for (1) 60 minutes and (2) 6 days.

At this condition, the concentration of the hydrogen ions in neutral water (pH = 7) is 10^{-7} mol. The anodic reaction that causes the dissolution of Mg occurs once the metal is in contact with the test electrolyte according to [33];

$$2Mg = 2Mg^{2+} + 4e^- \quad (3)$$

The anodic reaction also includes the formation of magnesium oxide as follows;

$$Mg + O = MgO \quad (4)$$

Because of secondary reactions, magnesium cations (reactions 3) will react with the hydroxide ions produced in reaction (2) as follows;

$$Mg^{2+} + 2OH^{-} = Mg(OH)_2 \quad (5)$$

According to Bender et al. [29], the equilibrium between water of the electrolyte and its ions is disturbed and the reaction becomes stronger in one direction (principle of Le Chatelier);

$$H_2O = (OH^{-})_{Mg} + H^{+} \quad (6)$$

It is clearly seen from Fig. 1 (curve 1) that an active dissolution of the alloy occurred with increasing potential in the anodic side under the aggressiveness action of the chloride ions presented in the test solution. Reversing the direction of potential led to further increases in the current and intersected with the cathodic branch indicating that the alloy suffers sever pitting corrosion and its protection potential is more negative than the corrosion potential. Increasing the immersion time to 6 days (curve 2) highly decreased the values of cathodic, j_{Corr}, and anodic currents, shifted E_{Corr} and E_{Prot} to the less negative direction, increased R_P, and decreased K_{Corr}. This indicates that the longer the exposure period the less the uniform corrosion of the Mg alloy in the test solution. According to Pardo et al. [34] the main corrosion product formed on the Mg surface after 10 days immersion in 3.5% NaCl was $Mg(OH)_2$, which provide partial protection to the alloy. On the other hand, this effect increased the pitting corrosion as the area of the hysteresis loop that appears on both curves is much bigger for Mg after 6 days immersion in the Cl^- solution before measurement. This was further confirmed by calculating the values of the cathodic (β_c) and anodic (β_a) Tafel slopes, E_{Corr}, j_{Corr}, E_{Prot}, R_P, and K_{Corr} from polarization curves shown in Fig. 1 and recorded in Table 1. The values of E_{Corr} and j_{Corr} were obtained from the extrapolation of anodic and cathodic Tafel lines located next to the linearized current regions. The values of E_{Prot} were determined from the backward anodic polarization curve at the intersection point with the forward polarization curve. The values of R_P and K_{Corr} were calculated from the polarization data as follows [35–37]:

$$R_P = \frac{1}{j_{Corr}} \left(\frac{\beta_c . \beta_a}{2.3(\beta_c + \beta_a)} \right) \quad (7)$$

$$K_{Corr} = \frac{j_{Corr}\, k\, E_W}{d\, A} \quad (8)$$

Where, j_{Corr} is the corrosion current density, β_c and β_a are the cathodic and anodic Tafel slopes, respectively, k is a constant that defines the units for the corrosion rate (= 3272 mm/ (amp.cm.year)), E_W the equivalent weight in grams/equivalent of Mg alloy (E_W = 12.15 grams/equivalent), d the density in g cm^{-3} (= 1.74), and A the area of the exposed surface of the electrode in cm^2.

Fig. 2 shows the CPP curves obtained for Mg electrode after its immersion in freely aerated 3.5% NaCl solutions for (a) 60 minutes and (b) 6 days without APT (1) and with $1x10^{-3}$ M APT (2) and $5x10^{-3}$ M APT (3). The corrosion parameters obtained from these curves in addition to the values

of the inhibition efficiency (*IE%*) are listed in Table 2. The *IE%* values for APT presented Table 2 were calculated according to the relation [38],

$$IE\% = \frac{j^{A}_{Corr} - j^{P}_{Corr}}{j^{A}_{Corr}} X100 \qquad (9)$$

Where, j^{A}_{Corr} and j^{P}_{Corr} are the corrosion currents in absence and presence of APT, respectively. It is seen from Fig. 2 and Table 2 that the cathodic and anodic currents and j_{Corr} significantly decreased in the presence of APT and upon the increase of its concentration. Also, the values of E_{Corr} increased to the more negative values, while E_{Prot} slightly shifted towards the positive direction. This effect also increased the values of R_P and decreased the values of corrosion rate K_{Corr}. The slight negative shift in the values of E_{Corr} in the presence of APT is apparently due to decreasing the rate of the cathodic reactions (reaction (1)).

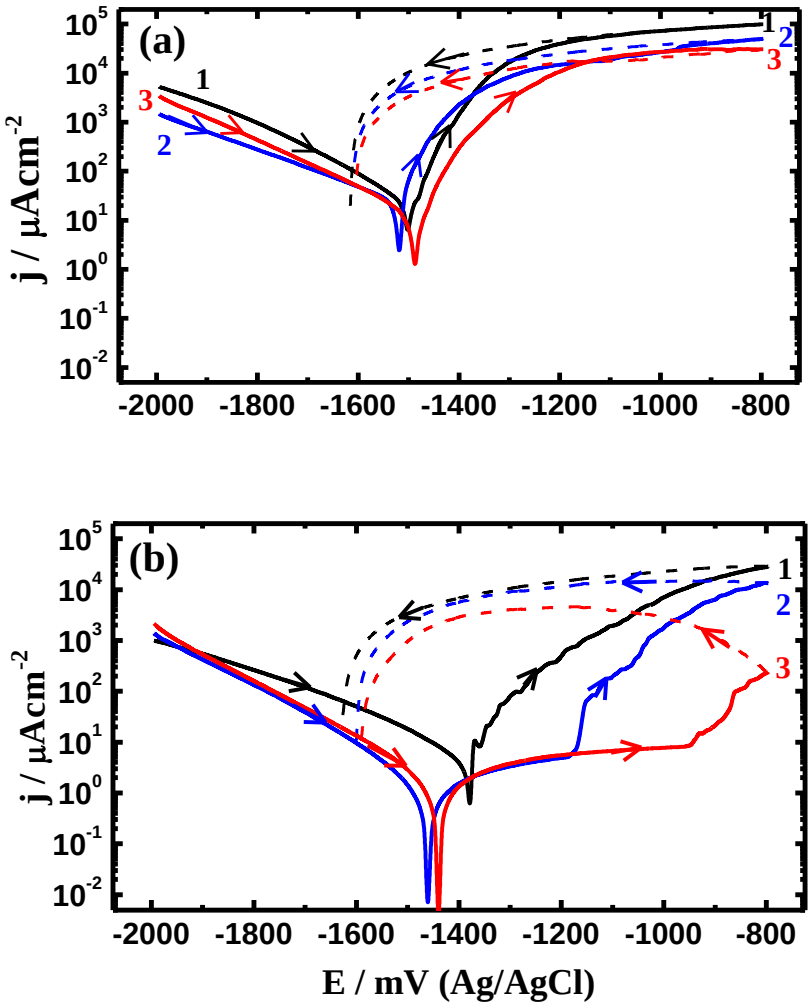

Figure 2. CPP curves obtained for Mg electrode after its immersion in freely aerated 3.5% NaCl solutions for (a) 60 minutes and (b) 6 days; (1) without APT, (2) with $1x10^{-3}$ M APT and (3) with $5x10^{-3}$ M APT.

Table 2. Corrosion parameters obtained from cyclic potentiodynamic polarization curves shown in Fig. 1 and Fig. 2 for the Mg electrode in aerated 3.5% NaCl solutions in absence and presence of APT.

Solution	Parameter							
	E_{Corr} / mV	j_{Corr} / μA cm^{-2}	β_c / mV dec^{-1}	β_a / mV dec^{-1}	E_{Prot} / mV	R_p / Ω cm^2	K_{Corr} / mmy^{-1}	IE / %
3.5% NaCl–60 min	–1513	33	175	63	–1615	0.610	0.754	–
+ $1x10^{-3}$ M APT	–1535	19	255	65	–1610	0.979	0.525	42.42
+ $5x10^{-3}$ M APT	–1495	13	185	67	–1605	1.645	0.297	60.61
3.5% NaCl–6 days	–1405	8.5	240	105	–1622	3.736	0.194	–
+ $1x10^{-3}$ M APT	–1460	0.9	140	240	–1600	42.75	0.021	89.2
+ $5x10^{-3}$ M APT	–1450	0.7	105	240	–1590	45.37	0.016	91.7

The decreases in cathodic and anodic currents and j_{Corr} and K_{Corr} in the presence of APT and with increasing its concentration are mainly due to the decrease of the chloride ion attack on the surface. The increase of RP and IE% with APT concentration resulted from the increased resistance of the Mg alloy against corrosion. It is also seen that the increase of immersion time from 60 min to 6 days further decreased the corrosion parameters and increased the inhibition efficiency of the APT molecules.

3.2. Chronoamperometric current–time measurements

The variation of the anodic dissolution currents versus time for Mg electrode that was immersed in the aerated 3.5% NaCl solutions in absence (1) and presence of (2) $1x10^{-3}$ M APT and (3) $5x10^{-3}$ M APT for 60 min (a) and 6 days (b), respectively before stepping the potential to –1200 mV vs. Ag/AgCl are shown in Fig. 3.

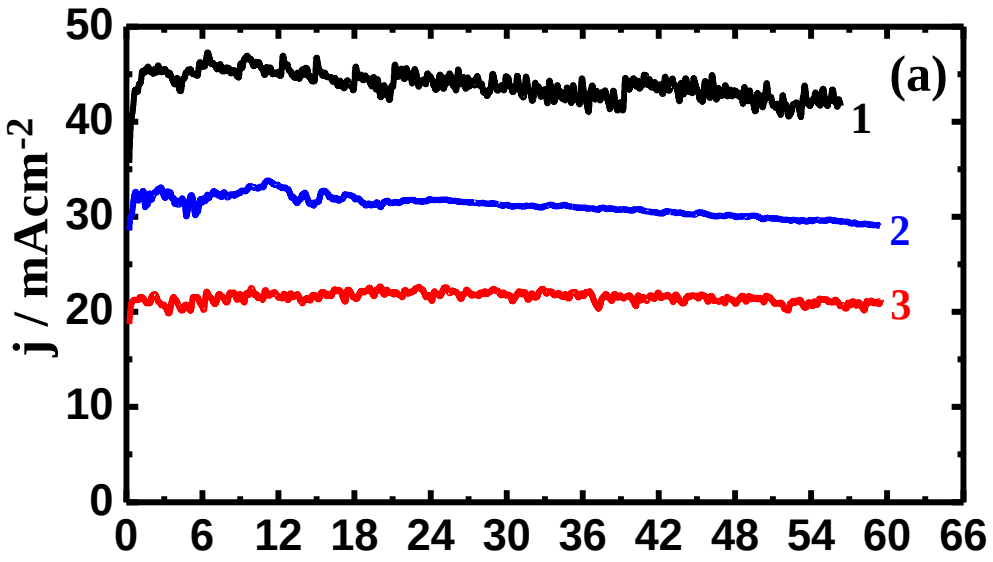

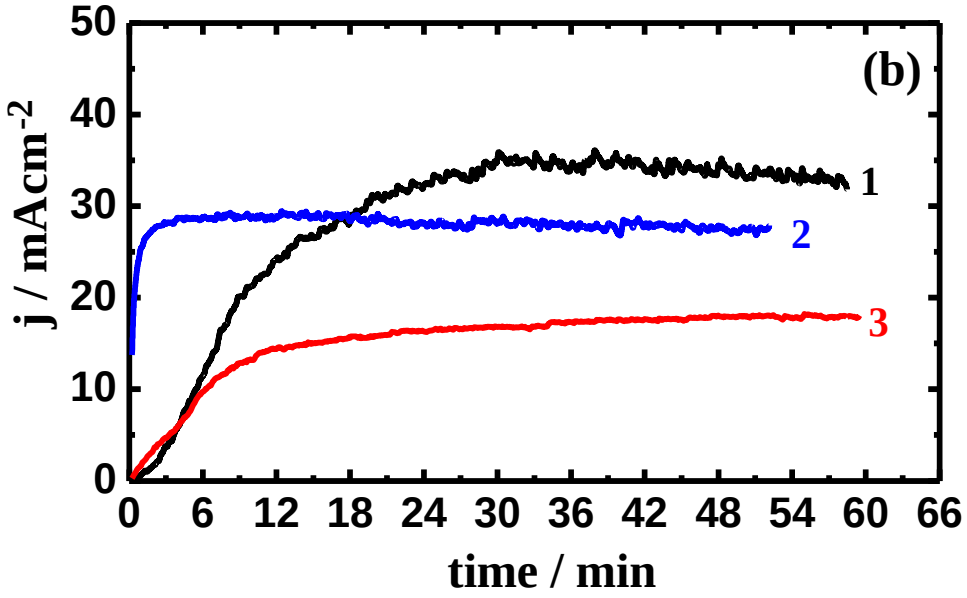

Figure 3. Chronoamperometric current-time curves obtained at constant potential of –1.2 V (Ag/AgCl) for Mg electrode after its immersion in freely aerated 3.5% NaCl solutions for (a) 60 minutes and (b) 6 days; (1) without APT, (2) with $1x10^{-3}$ M APT and (3) with $5x10^{-3}$ M APT.

These measurements were carried out in order to study both the general and pitting corrosion of Mg after varied exposure periods in the stagnant chloride solutions at a more anodic potential value. The value of the constant potential (–1200 mV) was determined from polarization curves. The highest current values for Mg were recorded when the measurements were carried out after 60 min of the electrode immersion, Fig. 3a, curve 1. In this case the current showed a rapid increase in its initial values due to the dissolution of an oxide film might have formed on the surface of the Mg alloy during its immersion in the test solution. The current then slightly increased and decreased accompanied by small fluctuations with a slow and slight absolute current decrease at the end of the run. This current behavior indicates that the Mg alloy suffers pitting corrosion. Increasing the immersion time to 6 days (Fig. 3b, curve 1) led to decreasing the initial current values to almost zero. This can be explained by the formation of a passive oxide film and/or corrosion products, which get thicker with time before applying the constant potential and then partially protect the Mg surface against general corrosion. The current then gradually increased with increasing the time of the experiment up to the first 40 min of the applied potential indicating on the occurrence of pitting corrosion. Where, pits develop at sites where, oxygen adsorbed on the alloy surface is displaced by an aggressive species such as Cl^- ions that are presented in the solution. This is because Cl^- ions have small diameters allows it to penetrate through the protective oxide film and displace oxygen at the sites where metal-oxygen bond is the weakest [39].

In the presence of $1x10^{-3}$ M APT after 60 min (Fig. 3a, curve 2) led to the decrease of the absolute current of Mg, which might be due to the increase of surface compactness by APT molecules. This effect increased with increasing the immersion time before measurement to 6 days (Fig. 3b, curve 2), where the APT molecules incorporated within the oxide film and/or corrosion products and made

Mg provided lower absolute current with time. Further increasing the APT concentration to $5x10^{-3}$ M decreased the absolute current and provided no fluctuations on the current curves. This indicates that the presence of APT and the increase of its concentration decreased the Mg uniform and pitting corrosion in the chloride test solution.

3.3. EIS measurements

The EIS measurements were carried out to determine kinetic parameters for electron transfer reactions at the Mg/electrolyte interface and to confirm the data obtained by polarization and chronoamperometric measurements. The Nyquist plots for Mg electrode at an open-circuit potential after its immersion in freely aerated 3.5% NaCl solutions without APT (1), with $1x10^{-3}$ M APT (2) and $5x10^{-3}$ M APT (3) for 60 minutes (a) and 6 days (b), respectively are shown in Fig. 4.

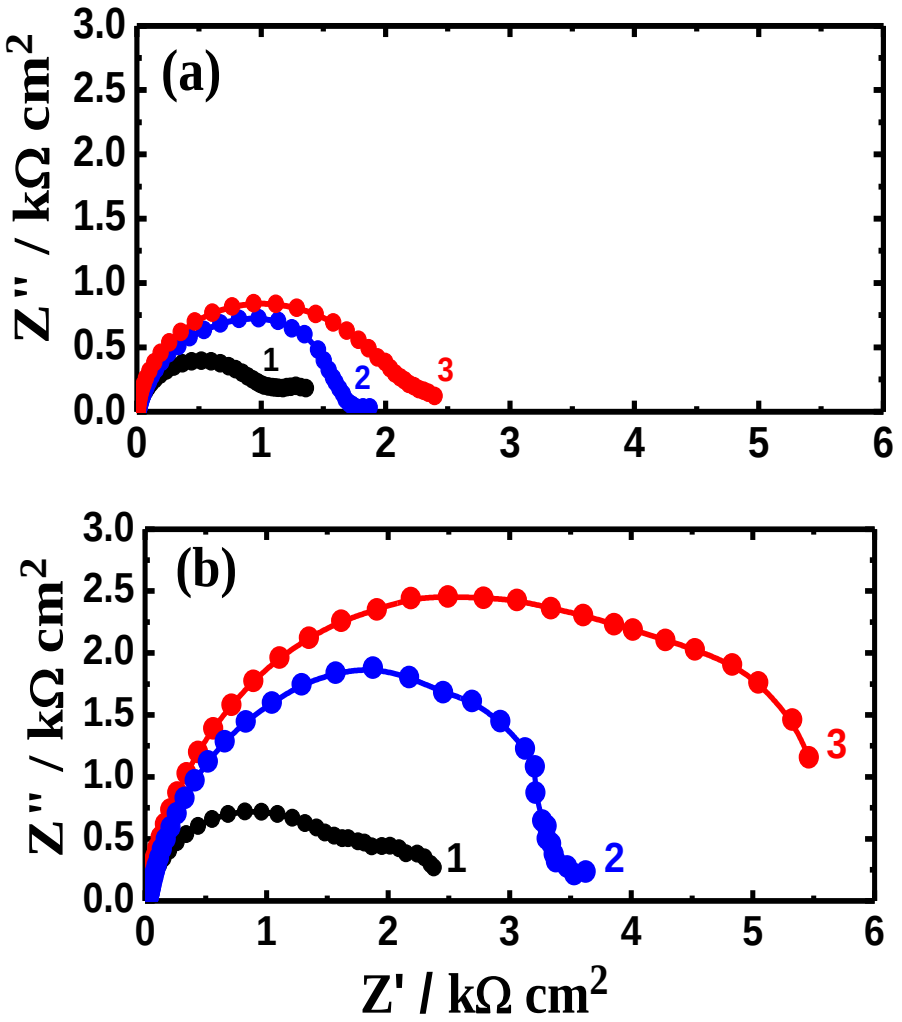

Figure 4. Nyquist plots for Mg electrode at an open-circuit potential after its immersion in freely aerated 3.5% NaCl solutions for (a) 60 minutes and (b) 6 days; (1) without APT, (2) with $1x10^{-3}$ M APT and (3) with $5x10^{-3}$ M APT.

The impedance spectra of the Nyquist plots were analysed by fitting to the equivalent circuit model shown in Fig. 5.

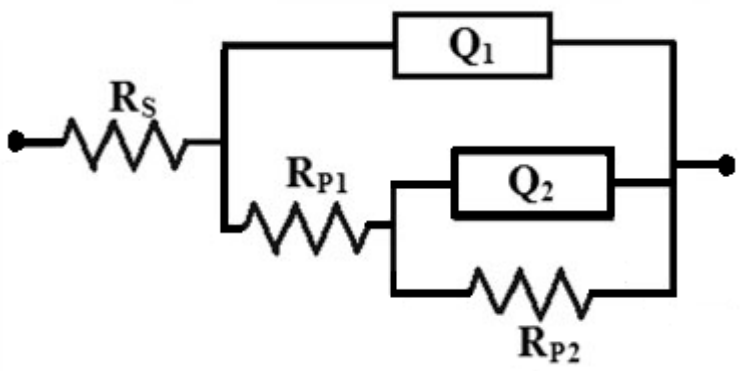

Figure 5. Equivalent circuit model used to fit the EIS experimental data presented in Fig. 4. See text for symbols used in the circuit.

The parameters obtained by fitting the equivalent circuit shown in Fig. 5, in addition to the values of IE% are listed in Table 3. Here, R_S represents the solution resistance between the alloy and the counter (platinum) electrode, Q_1 and Q_2 the constant phase elements (CPEs), R_{P1} the resistance of a film layer formed on the Mg alloy surface, and R_{P2} accounts for the polarization resistance at the alloy surface. The semicircles at high frequencies in Fig. 4 are generally associated with the relaxation of electrical double layer capacitors and the diameters of the high frequency semicircles can be considered as the charge transfer resistance ($R_P = R_{P1} + R_{P2}$) [14]. The values of IE% obtained by EIS were calculated from the charge transfer resistance as following [23];

$$IE\% = \frac{R_P - R_P^0}{R_P} X100 \qquad (10)$$

where R_P and R^0_P are the charge transfer resistances in chloride solution with and without APT, respectively. The IE% values increase upon addition of APT in all solutions, and the effect is enhanced when the APT concentration is increased (Table 3), which is also in agreement with results obtained by potentiodynamic polarization (Table 2).

It is seen from Fig. 4, Fig. 5, and Table 3 that the values of R_S, R_{P1} and R_{P2} increased in the presence of APT and up on the increase of its concentration. The polarization resistance here is a measure of the uniform corrosion rate as opposed to tendency towards localized corrosion. This effect was noticed to also increase with increasing the exposure time of the alloy to 6 days before measurement. The CPEs, Q_1 and Q_2 with their n values close to 1.0 (Table 3) represent double layer capacitors with some pores; the CPEs decrease, while their *n*-values increase upon addition of APT and upon increase in its concentration, which are expected to cover the charged surfaces reducing the capacitive effects.

Table 3. EIS parameters obtained by fitting the Nyquist plots shown in Fig. 4 with the equivalent circuit shown in Fig. 5 for magnesium electrodes after 60 min and 6 days of immersion in aerated 3.5% NaCl solutions in absence and presence of APT.

Solution	Parameter							
	R_S / Ωcm^2	Q_1		R_{P1} / Ω cm^2	Q_2		R_{P2} / Ω cm^2	IE / %
		Y_{Q1} / µF cm^{-2}	n		Y_{Q2} / µF cm^{-2}	n		
3.5% NaCl (60 min)	8.420	0.205	0.80	320	1.058	0.11	629	–
+ $1x10^{-3}$ M APT (60 min)	11.34	0.145	0.89	970	0.766	0.86	1746	65.06
+ $5x10^{-3}$ M APT (60 min)	17.10	0.086	1.00	1161	0.339	0.93	2127	71.14
3.5% NaCl (6 days)	16.36	0.153	0.89	547	0.805	0.67	884	–
+ $1x10^{-3}$ M APT (6 days)	21.26	0.083	0.90	1981	0.475	0.81	2125	65.14
+ $5x10^{-3}$ M APT (6 days)	27.49	0.021	0.92	2348	0.258	1.00	2963	73.06

This was indicated also by the increase of the diameter of the measured EIS curves with APT and exposure time. The increase of resistances of Mg with APT concentration is due to the adsorption of its molecules to repair the flawed parts on the alloy surface due to the chloride ions attack. Whereas, the increase of the resistance with immersion time is attributed to the formation of a partially passive film and/or corrosion products that get thicker with exposure time and could lead to the decrease in j_{Corr} and K_{Corr} and also the increase in R_P values we have seen in polarization data (Fig. 1, Fig. 2 and Table 2) under the same conditions.

3. 4. Weight-loss data, SEM / EDX investigations and inhibition efficiency

The variations of (a) weight loss (ΔW, $g.cm^{-2}$) and (b) corrosion rate (K_{Corr}, mmpy), respectively with time in 25 days for Mg coupons in 300 cm^3 of aerated stagnant 3.5% NaCl solutions are shown in Fig. 6. The values of ΔW and K_{Corr} were calculated as follows [14]:

$$\Delta W = \frac{W_1 - W_2}{A} \quad (11)$$

$$K_{Corr} = \frac{\Delta W * K}{D * t} \quad (12)$$

Where, W_1 and W_2 are the weighs of magnesium coupon per gram before and after its immersion in the test solution, A is the area of magnesium coupon per cm^2, K is a constant that defines the unit of the corrosion rate (K = 8.76 x 10^4 for the mmpy unit), D is the density of magnesium per g/cm^3 and t is the immersion time per hour.

It is obvious from Fig. 6a (curve 1) that the values of ΔW for Mg in Cl^- solutions alone increased with time due to the continuous aggressiveness attack of the chloride ions to t the alloy surface. On the other hand, the K_{Corr} values (Fig. 6b, curve 1) decreased with time due to the

accumulation of corrosion products including magnesium oxide and chloride, which cover up the surface and decreases its uniform corrosion rate. The presence of $1x10^{-3}$ M APT (curves 2) decreased both ΔW and K_{Corr} values due to the protective action of APT molecules that reduces the attack of Cl^- ions on the Mg surface. This effect greatly increased upon the increase of APT concentration to $5x10^{-3}$ M, which recorded the minimum ΔW and K_{Corr} values. The gravimetric data here are in good agreement with those ones obtained from polarization, chronoamperometry, and EIS we have seen earlier.

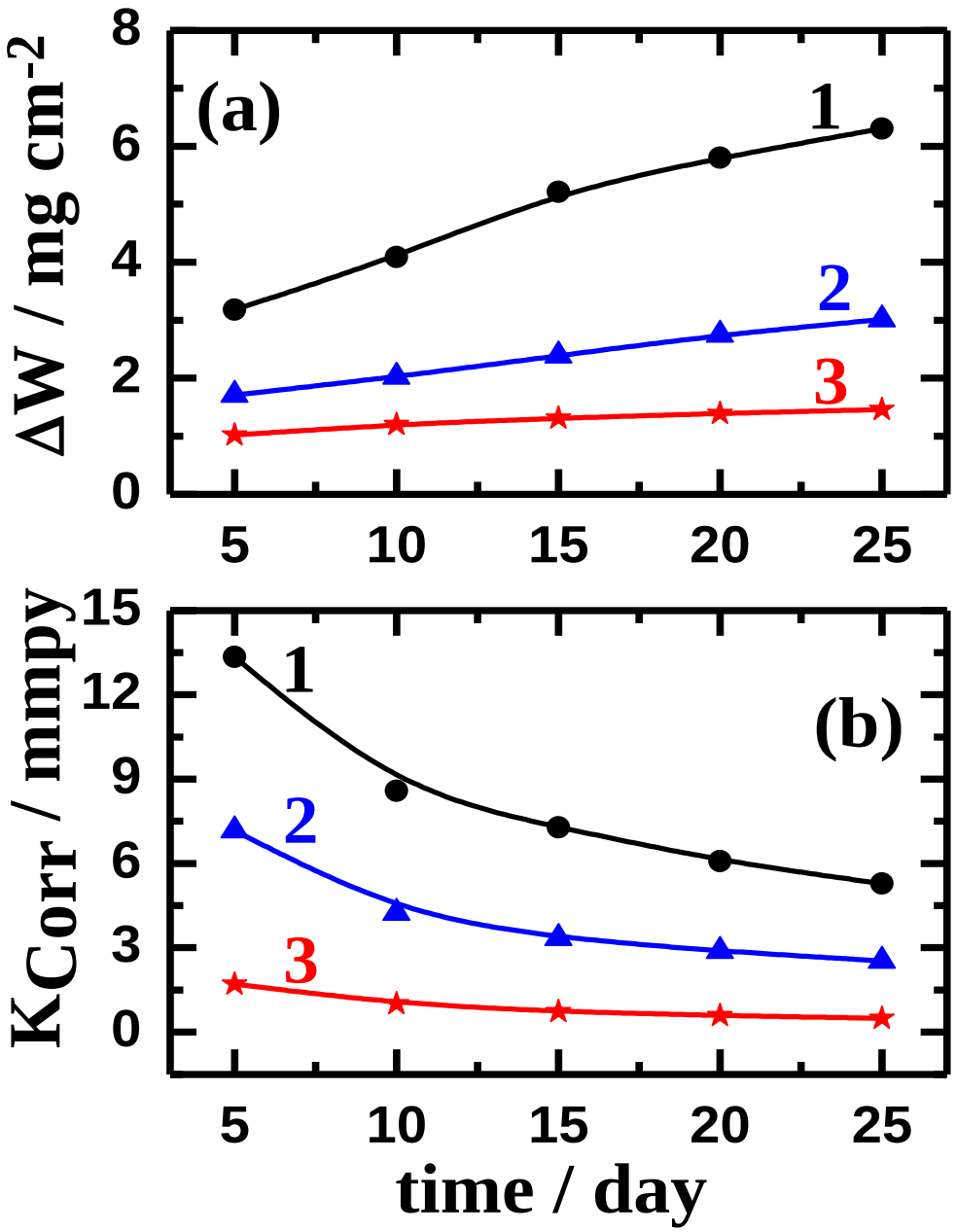

Figure 6. Variations of the (a) weight loss (ΔW / mg.cm^{-2}) and (b) corrosion rate (K_{Corr} / mmpy), with time for Mg coupons in 3.5% NaCl solutions; (1) without APT, (2) with $1x10^{-3}$ M APT and (3) with $5x10^{-3}$ M APT.

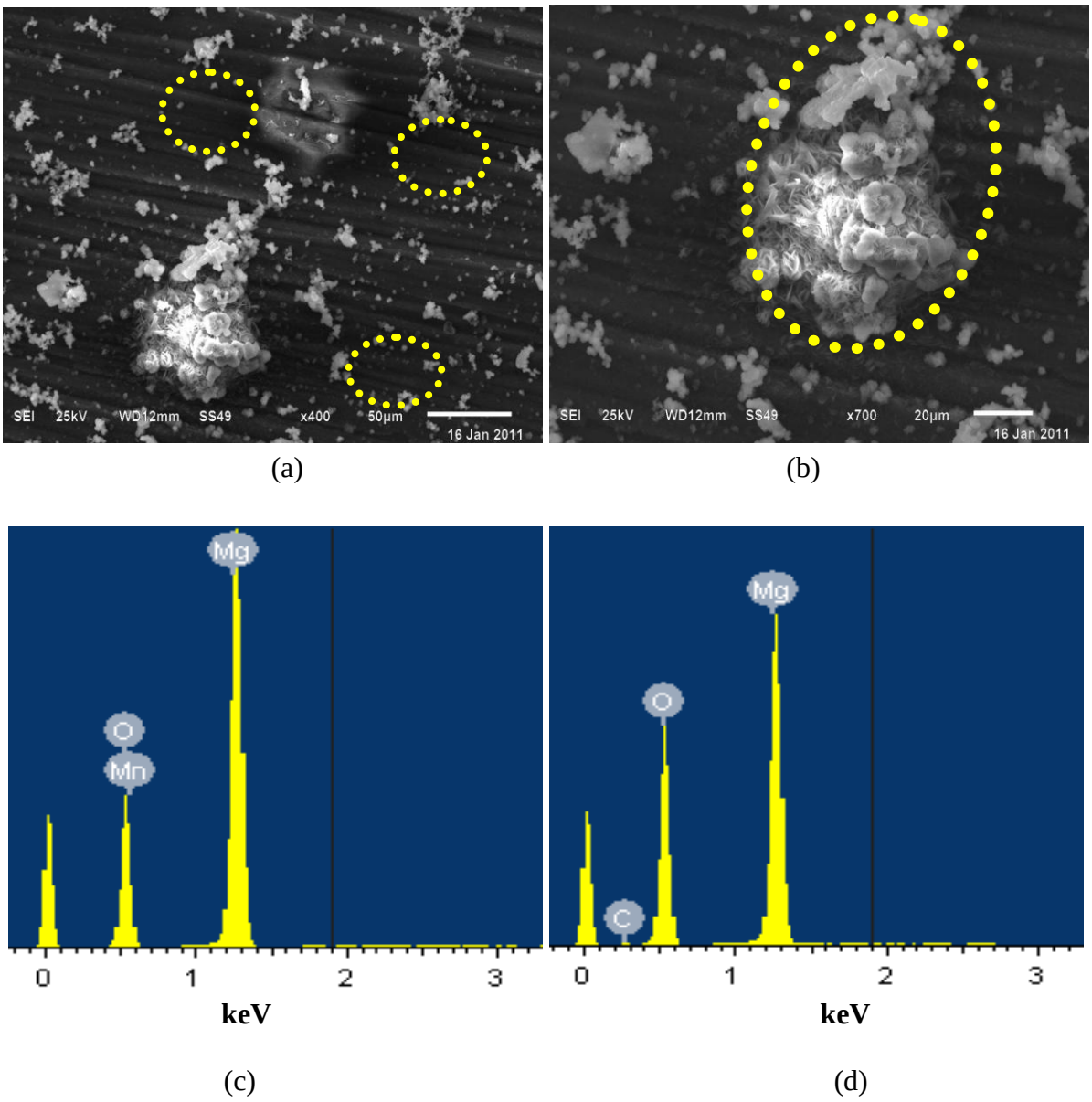

Figure 7. SEM micrographs (a) and (b) at different magnifications for Mg surface after its immersion in 3.5 NaCl solutions for 25 days; and the corresponding EDX profile analyses taken in the selected SEM areas represented by (c) and (d), respectively.

In order to differentiate between the surface morphology and to identify the composition of the species formed on the magnesium surface after its immersion in aerated 3.5% NaCl in absence and presence of APT, SEM/EDX investigations were carried out. Fig. 7 shows the SEM micrographs of (a) a large area of the surface, (b) an extended area contains white deposits for Mg surface after its immersion for 25 days in 3.5% NaCl solution. The corresponding EDX profile analyses for the selected areas on the SEM images (a) and (b) are shown in Fig. 7c and Fig. 7d, respectively. It is clearly seen from the SEM images that there are black and white areas with shaped like pit observed on the Mg surface. The atomic percentage of the elements found in the selected black areas shown in Fig. 8a and displayed in the EDX profile presented in Fig. 8c, were 55.74% O, 41.76% Mg, 2.40% C, and 0.11% Mn. This suggests that the compounds formed on the Mg alloy in black areas are mainly

magnesium oxide. On the other hand, the atomic percentages of the elements found in the white area of SEM image shown in Fig. 8b and displayed in the EDX profile depicted in Fig. 8d, were 65.86% O, 30.14% Mg, and 4.00% C. this means that the oxide film in the white areas are more dense than the black areas as the percentage of O is higher.

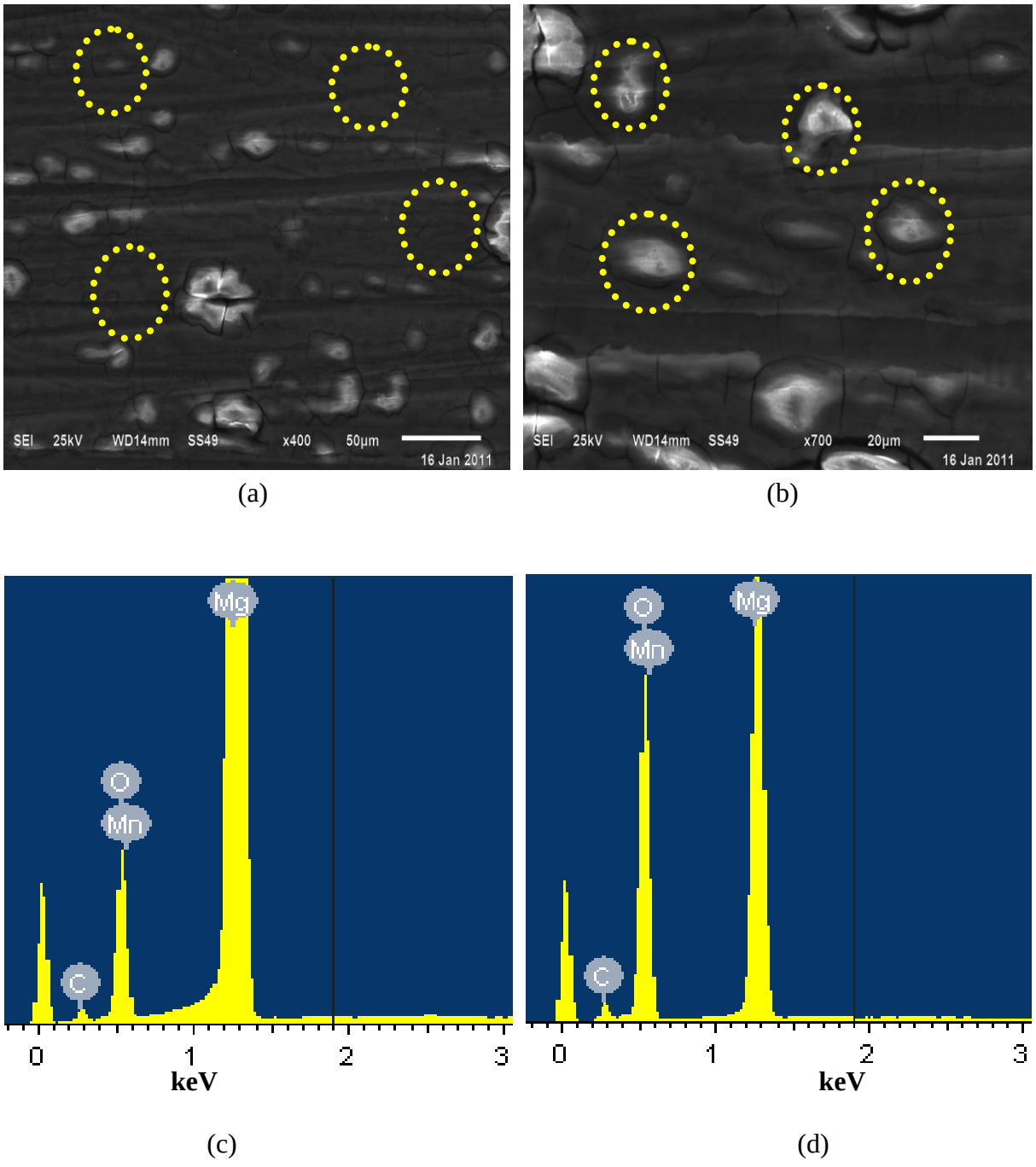

Figure 8. SEM micrographs (a) and (b) with different scales for Mg surface after its immersion in 3.5 NaCl + 10^{-3} M APT solutions for 25 days; and the corresponding EDX profile analyses taken in the selected SEM areas represented by (c) and (d), respectively.

The SEM micrographs with different scales for Mg surface after its immersion in 3.5 NaCl + 10^{-3} M APT solutions for 25 days are depicted in Fig. 8a and Fig. 8b, while the corresponding EDX profile analyses taken in the selected SEM areas represented by Fig. 8c and Fig. 8d, respectively. The SEM images here show homogenous surface that contains some white areas. The atomic percentage of the elements found in the major investigated surface area (black) marked in Fig. 8a and represented by the EDX profile shown in Fig. 8c were 25.47% O, 64.26% Mg, 12.05% C, and 0.24% Mn and indicated that magnesium oxide is existing in this area. The elements found in the selected white areas on the SEM image (b) and shown in the EDX spectrum (d) were 60.56% O, 24.12% Mg, 14.96% C, and 0.36% Mn. The content of O in here is higher than in the black area. The high content of carbon compound might have existed due to the adsorption of APT compound onto Mg during its immersion in the test solution.

The change of the inhibition efficiency (*IE%*) with time for Mg coupons in 3.5% NaCl solutions by $1x10^{-3}$ and $5x10^{-3}$ M APT, respectively is shown in Fig. 9.

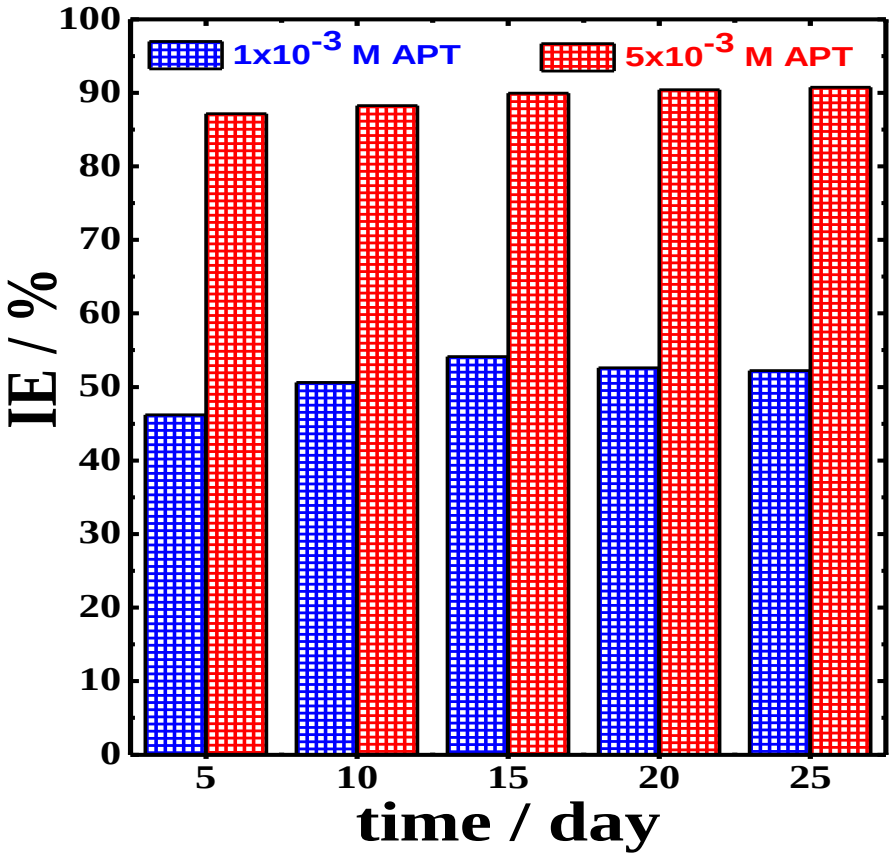

Figure 9. Change of the inhibition efficiency (*IE%*) with time for Mg coupons in 3.5% NaCl solutions by $1x10^{-3}$ and $5x10^{-3}$ M APT, respectively.

The IE% values were calculated from the loss in weight data as reported in our previous work [40]. It is seen that the inhibition efficiency stays about 47–55% for a 25 day period in the presence of $1x10^{-3}$ M APT, while it is somewhere between 88% and 91% with $5x10^{-3}$ M.

4. CONCLUSIONS

The corrosion and corrosion inhibition of Mg/Mn alloy in 3.5% NaCl solutions by 5-(3-aminophenyl)-tetrazole (APT) after different exposure intervals have been investigated using cyclic potentiodynamic polarization (CPP), chronoamperometric current-time (CT) and impedance spectroscopy (EIS) measurements after 60 min and 6 days. The study was complemented by weight-loss data after exposure periods varied from 5 to 25 days, scanning electron microscopy (SEM) and X-ray analyzer (EDX) investigations. Electrochemical measurements indicated that the dissolution of Mg/Mn alloy decreased in the presence of APT and the increase of its concentration. Increasing the immersion time from 60 min to 6 days before measurements also decreased the uniform corrosion, while increase the pitting attack for the alloy. Gravimetric measurements confirmed that APT inhibited the uniform corrosion of the alloy and its efficiency increases with the increase of its concentration and exposure time. It also confirmed that the immersion time decreases the uniform corrosion of Mg even in absence of APT molecules. The SEM/EDX investigations after 25 days immersion in chloride solutions with and without APT provided another prove that APT molecules precluded the corrosion of Mg through their adsorption onto the surface to repair its flawed parts, which in turn lowered the corrosivity of the test chloride solution.

ACKNOWLEDGEMENTS
The authors extend their appreciation to the Deanship of Scientific Research at KSU for funding the work through the research group project No. RGP-VPP-160.

References

1. K. U. Kainer, F. Kaiser, Eds. *Magnesium alloys and technology*, Weinheim: Wiley-VCH GmbH (2003).
2. A.R. Shashikala, R. Umarani, S. M. Mayanna, A. K. Sharma, *Int. J. Electrochem. Sci.,* 3 (2008) 993.
3. H. E. Friedrich, M. L. Mordike, Eds. *Magnesium technology*, Springer-Verlag, Berlin, Heidelberg (2006).
4. M. Hakamada, T. Furuta, Y. Chino, Y. Q. Chen, H. Kusuda, M. Mabuchi, *Energy*, 32 (2007) 1352.
5. G.L. Song, A. Atrens, *Advanced Engineering Materials*, 5 (2003) 837.
6. G. Song, A. Atrens, *Advanced Engineering Materials*, 1 (1999) 11.
7. G. T. Parthiban, K. Bharanidharan, D. Dhayanand, Thirumalai Parthiban, N. Palaniswamy, V. Sivan, *Int. J. Electrochem. Sci.,* 3 (2008) 1162.
8. G. Song, *Advanced Engineering Materials*, 7 (2005) 563.
9. Anna Da Forno, Massimiliano Bestetti, *Advanced Research Materials*, 138 (2010) 79.
10. S. Yu. Kondrat'ev, G. Ya. Yaroslavskii, B. S. Chaikovskii, *Strength of Materials*, 18 (1986) 1325.
11. M. Carboneras, L. S. Hernandez, J. A. del Valle, M. C. Garcia-Alonso, M. L. Escudero, *J. Alloys Compd.*, 496 (2010) 442.
12. J. Kim, K. C. Wong, P. C. Wong, S. A. Kulinich, J. B. Metson, K. A. R. Mitchell, *Appl. Surf. Sci.,* 253 (2007) 4197.
13. F. Zucchi, V. Grassi, A. Frignani, C. Ponticelli, G. Trabanelli, *Surf. Coat. Technol.*, 20 (2006) 4136.
14. E. M. Sherif, S.-M. Park, *Corros. Sci.,* 48 (2006) 4065.

15. E. M. Sherif, A. A Almajid, *J. Appl. Electrochem.*, 40 (2010) 1555.
16. E. M. Sherif, *Int. J. Electrochem. Sci.* 6 (2011) 1479.
17. E. M. Sherif, A. H. Ahmed, *Synthesis and Reactivity in Inorganic, Metal-Organic, and Nano-Metal Chemistry*, 40 (2010) 365.
18. E. M. Sherif, R. M. Erasmus, J. D. Comins, *Electrochim. Acta*, 55 (2010) 3657.
19. E. M. Sherif, *J. Mater. Eng. Performance*, 19 (2010) 873.
20. F. Farelas, A. Ramirez, *Int. J. Electrochem. Sci.*, 5 (2010) 797.
21. A.Y. Musa, A. A. H. Kadhum, A. B. Muhamad, Int. *J. Electrochem. Sci.*, 5 (2010) 1911.
22. X. Joseph Raj, N. Rajendran, *Int. J. Electrochem. Sci.*, 6 (2011) 348.
23. E. M. Sherif, R. M. Erasmus, J. D. Comins, *Corros. Sci.*, 50 (2008) 3439.
24. O. L. Riggs Jr., *Corrosion Inhibitors*, second ed., C. C. Nathan, Houston, TX, 1973.
25. G. Song, D. H. StJohn, *Mater. Corros.*, 56 (2005) 15.
26. G. Song, The corrosion and protection of magnesium alloys, *Chemical Industry Press of China*, ISBN 7-5025-8565-6, Beijing (2006).
27. A.F. Galio, S. V. Lamaka, M. L. Zheludkevich, L. F. P. Dick, I. L. Müller, M. G. S. Ferreira, *Surf. Coat. Technol.*, 204 (2010) 1479.
28. Adel Mesbah, Caroline Juers, Françoise Lacouture, Stéphane Mathieu, Emmanuel Rocca, Michel François, Jean Steinmetz, *Solid State Sci*. 9 (2007) 322.
29. Xu Yang, Fu Sheng Pan, Ding Fei Zhang, *Mater. Sci. Forum*, 610–613 (2009) 920.
30. E. M. Sherif, R. M. Erasmus, J. D. Comins, *J. Appl. Electrochem.* 39 (2009) 83–91.
31. E. M. Sherif, Effects of 5-(3-aminophenyl)-tetrazole on the inhibition of unalloyed iron corrosion in aerated 3.5% sodium chloride solutions as a corrosion inhibitor, Accepted for publication, *Mater. Chem. Phys.* (2011).
32. S. Bender, J. Goellner, A. Heyn, E. Boese, *Mater. Corros.*, 58 (2007) 977-982.
33. Zhiming Shi, Andrej Atrens, *Corros. Sci*,. 53 (2011) 226–246.
34. A.Pardo, M.C. Merino, A. E. Coy, R. Arrabal, F. Viejo, E. Matykina, *Corros. Sci.* 50 (2008) 823.
35. E. M. Sherif, J. H. Potgieter, J. D. Comins, L. Cornish, P. A. Olubambi, C. N. Machio, *J. Appl. Electrochem.*, 39 (2009) 1385.
36. E. M. Sherif, J. H. Potgieter, J. D. Comins, L. Cornish, P. A. Olubambi, C. N. Machio, *Corros. Sci.*, 51 (2009) 1364.
37. E. M. Sherif, A. A. Almajid, F. H. Latif, H. Junaedi, *Int. J. Electrochem. Sci.*, 6 (2011) 1085.
38. E. M. Sherif, S.-M. Park, *Electrochim. Acta*, 51 (2006) 4665–4673.
39. Z. Szklarska-Smialowska, editor. *Pitting Corrosion of Metals*, NACE International, Houston (1986).
40. E. M. Sherif, S.-M. Park, *Electrochim. Acta*, 51 (2006) 6556–6562.